DOE/ET-53088-196 IFSR #196

ENERGY CONFINEMENT IN A HIGH-CURRENT REVERSED FIELD PINCH

Z.G. An
G.S. Lee
P.H. Diamond

Institute for Fusion Studies
The University of Texas at Austin
Austin, Texas 78712

July 1985

196

Energy Confinement in a High-Current Reversed Field Pinch

Z.G. An, G.S. Lee, and P.H. Diamond

Institute for Fusion Studies

The University of Texas at Austin

Austin, Texas 78712

Abstract

The ion temperature gradient driven (η_i) mode is proposed as a candidate for the cause of anomalous transport in high current reversed field pinches. A 'four-field' fluid model is derived to describe the coupled nonlinear evolution of resistive interchange and η_i modes. A renormalized theory is discussed, and the saturation level of the fluctuations is analytically estimated. Transport scalings are obtained, and their implications discussed. In particular, these results indicate that pellet injection is a potentially viable mechanism for improving energy confinement in a high temperature RFP.

Invited Presentation at the 7th Symposium on Compact Toroid Research, May 21-23, 1985, Santa Fe, New Mexico.

I. Introduction

In present temperature and current regimes, the resistive interchange (g) mode is a good candidate for the cause of anomalous transport in the Reversed Field Pinch. This mode may also play a role in thermal transport in spheromaks. A theory[1,2] of g-mode turbulence predicts saturation at a level of convective diffusion of pressure consistent with a mixing length estimate, which is: $D_{\text{conv}} \equiv \sum_{\mathbf{k}'} k_y'^2 |\tilde{\phi}_{\mathbf{k}'}|^2 / \Delta\omega_{\mathbf{k}''} = L_s^2 \eta \kappa \beta_\theta / L_p$. Here $\kappa = 1/R_c \sim 1/a$ refers to curvature, η is the resistivity, and L_p is the pressure gradient. The associated magnetic fluctuation $\delta B_r/B \sim \beta_\theta^{4/3} S^{-2/3}$ causes thermal conduction losses with conduction coefficient $\chi_E = (1/4\pi)^{1/2}(\epsilon/q'a)^3 \beta_\theta^{3/2} v_{Te} a/S$, where $\epsilon = a/R$, q is the safety factor, v_{Te} is the electron thermal speed, and $S = (\tau_R/\tau_{A\theta})$ is the inverse Lundquist number. Balancing thermal losses with Ohmic heating indicates a constant $\beta_\theta \cong (q'a/\epsilon)(m_e/m_i)^{1/6} \sim 10\%$, and the scaling $T_e \sim I_p^2/N$.[1,2,3] This result is in good accord with that observed in current RFP experiments. However, a crucial underlying assumption of the resistive MHD theory is non-adiabatic electron dynamics, namely that $\alpha \equiv k_\parallel^2 v_{Te}^2/\gamma\nu_e << 1$. Since $\alpha \propto T^{5/3} n^{-2/3} B_\theta^{-2/3}$, it is very likely that $\alpha > 1$ in proposed future RFP experiments. Indeed, for $ZT-40$, ($a = 20cm$, $B_\theta = 4k$ Gauss, $n = 0.6 \times 10^{14}/cm^3$, $T = 100 \sim 400ev$), $0.2 < \alpha < 2$. Using proposed $ZT-H$ parameters, ($a = 40cm$, $B_\theta = 10k$ Gauss, $n = 1.2 \times 10^{14}/cm^3$, $T = 2kev$), $\alpha \sim 4.2$. It is therefore important to consider adiabatic electron dynamics regimes. Furthermore, a rather broad density profile has been experimentally observed in RFP's. In addition, significant ion heating occurs because of anomalous processes *and* thermal equilibration ($\tau_{E\ \text{conf.}} \sim \tau_{E\ \text{equil}}$ at high current in $ZT-40$)[4]. Moreover, it is unlikely that magnetic stochasticity associated with dynamo activity will flatten the resulting ion temperature gradient. Thus, it is quite possible that the ion temperature gradient parameter $\eta_i = d\ell n T_i/d\ell n\ n$ is sufficient for the onset of ion temperature (pressure) gradient driven (η_i) instabilities. Since η_i-mode growth increases with magnetic shear strength (large in RFP where $L_s \sim L_p$), these instabilities appear to be strong candidates for the underlying cause of confinement degradation in high current RFP's. They are especially important in discharges where the macroscopic MHD activity is coherent. We are thus motivated to investigate the coupled resistive interchange (g)-ion temperature gradient driven (η_i) system[5] for RFP.

II. Model

Starting from the two-fluid theory[6], a four-field model to describe (coupled) nonlinear evolution of g and η_i (above threshold) modes was derived. The basic system is

$$\left[\frac{\partial}{\partial t} + (1+\eta_i)V_{Di}\frac{\partial}{\partial y} + \rho_s C_s \mathbf{b}\times\nabla\tilde{\phi}\cdot\nabla_\perp\right]\rho_s^2\nabla_\perp^2\tilde{\phi}$$

$$+ V_C\frac{\partial}{\partial y}\left[(1+\tau)(\tilde{h}+\tilde{\phi}) + \tilde{\tau}_i\right] - \frac{v_{Te}^2}{\nu_e}\nabla_\parallel^2\tilde{h} = 0 \tag{1}$$

$$\frac{\partial(\tilde{h}+\tilde{\phi})}{\partial t} + \rho_s C_s \mathbf{b}\times\nabla\tilde{\phi}\cdot\nabla_\perp\tilde{h} = -V_{De}\frac{\partial\tilde{\phi}}{\partial y} - \tau V_C\frac{\partial\tilde{h}}{\partial y} - \nabla_\parallel\tilde{v}_{\parallel i} + \frac{v_{Te}^2}{\nu_e}\nabla_\parallel^2\tilde{h} \tag{2}$$

$$\left(\frac{\partial}{\partial t} + \rho_s C_s \mathbf{b}\times\nabla\tilde{\phi}\cdot\nabla_\perp\right)\tilde{v}_{\parallel i} = -\frac{T_i}{m_i}\nabla_\parallel\left[(1+\tau)(\tilde{h}+\tilde{\phi}) + \tilde{\tau}_i\right] + \nabla_\parallel(\mu_\parallel\nabla_\parallel\tilde{v}_{\parallel i}) \tag{3}$$

$$\left(\frac{\partial}{\partial t} + \rho_s C_s \mathbf{b}\times\nabla\tilde{\phi}\cdot\nabla_\perp\right)\tilde{\tau}_i = -\frac{2}{3}\nabla_\parallel\tilde{v}_{\parallel i} - \eta_i V_{De}\frac{\partial\tilde{\phi}}{\partial y} \tag{4}$$

where $V_{Di,e} = \pm cT_{i,e}(d\ell n\ n/dx)/eB$, $V_c = cT_i/eBR_c$, $\rho_s = C_s/\Omega_i$, $C_s = (T_e/m_i)^{1/2}$, $\Omega_i = eB/mc$, $\tau = T_e/T_i$, and $\eta_i = d\ell n\ T_i/d\ell n\ n$. To simplify notation we have written $\tilde{\phi}$ for $e\phi/T_e$, $\tilde{n}$ for $\tilde{n}/n_0$, and $\tilde{\tau}_i$ for $\tilde{T}_i/T_i$. Here $\tilde{h} = \tilde{n} - \tilde{\phi}$ is the non-adiabatic part of the density fluctuation.

III. Conservation Relation

Define the total energy

$$E = \left\langle \frac{\rho_s^2}{2}\left|\nabla_\perp\tilde{\phi}\right|^2 + \frac{1}{2}\left|\tilde{h}+\tilde{\phi}\right|^2 + \frac{1}{2}\frac{m_i}{T_i+T_e}\left|\tilde{v}_{\parallel i}\right|^2 + \frac{3}{4}\frac{T_i}{T_i+T_e}\left|\tilde{\tau}_i\right|^2\right\rangle. \tag{5}$$

Noting the V_D and V_C terms contribute pieces odd in y, and using the property of the convective nonlinearity $\langle f\mathbf{b}\times\nabla\tilde{\phi}\cdot\nabla_\perp f\rangle = 0$, for any function f, we can directly prove the following conservation law from the basic equations:

$$\frac{\partial E}{\partial t} = -\frac{c}{eB}\left(\frac{T_i}{R_c} + \frac{3}{2}\frac{T_e}{(1+\tau)L_{Ti}}\right)\left\langle\tilde{\tau}_i\nabla_y\tilde{\phi}\right\rangle - \frac{v_{Te}^2}{\nu_e}\left\langle\left|\nabla_\parallel\tilde{h}\right|^2\right\rangle$$

$$-\frac{c}{eB}\left(\frac{T_i}{R_c} + \frac{T_e}{L_n}\right)\left\langle\tilde{h}\nabla_y\tilde{\phi}\right\rangle - \frac{1}{1+\tau}\left\langle\frac{\mu}{v_{Ti}^2}\left|\nabla_\parallel\tilde{v}_{\parallel i}\right|^2\right\rangle \tag{6}$$

where $L_{Ti} = -(d\ell n\ T_i/dx)^{-1}$, $L_n = -(d\ell n\ n/dx)^{-1}$, and $\mu_\parallel$ is the parallel ion viscosity (or Landau damping coefficient, in collisionless regimes). The source terms are in the form of radial fluxes $\left\langle\tilde{\tau}_i \nabla_y \tilde{\phi}\right\rangle$ and $\left\langle\tilde{h} \nabla_y \tilde{\phi}\right\rangle$ multiplied by curvature $(1/R_c)$, ion temperature gradient $(1/L_{Ti})$, and density $(1/L_n)$. One sink term is due to the resistive field line diffusion, the other is due to parallel ion viscosity (or Landau damping), which results in ion heating. In the pure g-mode limit $\tilde{j}_{\|} = (T_e/e\eta_{\|})\nabla_{\|}(-e\tilde{\phi}/T_e + \tilde{n}/n_0) \rightarrow \tilde{E}_{\|}/\eta_{\|}$, $\tilde{n} \sim (\omega_{*e}/\gamma)\tilde{\phi} < \tilde{\phi}$. In the pure η_i limit $\tilde{h} \rightarrow 0$. In the $\tilde{h} \rightarrow 0$ limit, the only significant source term is due to the flux $\left\langle\tilde{\tau}_i \nabla_y \tilde{\phi}\right\rangle$, to which curvature $(1/R_c)$ and temperature gradient $(1/L_{Ti})$ drives couple additively.

IV. Linear Instabilities

Linearization of (1)-(4) leads to the eigenmode equation

$$\rho_s^2\left[\omega + \omega_{*e}\frac{T_i}{T_e}(1+\eta_i)\right]\nabla_\perp^2\tilde{\phi} + (S/D)\tilde{\phi} = 0 \tag{7}$$

where $S = \omega_D\omega\left[(1+\tau)(\omega_{*e} - \omega_D\tau + iK_e) + (\omega_{*e}/\omega)\eta_i(\omega - \omega_D\tau + iK_e)\right] - iK_e\left[k_{\|}^2(\frac{5}{3}T_i + T_e)/m_i - \omega^2 + k_{\|}^2 T_i(\omega_{*e}/\omega)(\eta_i - \frac{2}{3})/m_i + \omega_{*e}\omega\right]$, $D = k_{\|}^2(\frac{5}{3}T_i + T_e)/m_i - \omega^2 + (iK_e - \omega_D\tau)(\frac{2}{3}k_{\|}^2 T_i/m_i\omega - \omega)$, $\omega_{*e} = ik_yV_{De}$, $\omega_D = ik_yV_C$, $K_e = k_{\|}^2 v_{Te}^2/\nu_e$. Equation (7) is solved numerically by a shooting code. Typical results are shown in Fig. 1-4. In Fig. 2 and 4, the potentials are defined as $(S/D)/[\omega + \omega_{*e}(1+\eta_i)T_i/T_e]$.

Analytical progress can be made in the pure η_i mode limit by noting $K_e = k_{\|}^2 v_{Te}^2/\nu_e \rightarrow \infty$, so that $\tilde{h} = \tilde{n} - \tilde{\phi} = 0$. For $\omega << \omega_{*e}$, the growth rate is $\gamma = (\eta_i + 1)^{1/2}(\eta_i - \frac{2}{3})^{1/2}k_y v_{Ti} a_i/L_s$, and the mode width is $\lambda = (1+\eta_i)^{1/2}a_i$, where $a_i = v_{Ti}/\Omega_i$. Shooting code results indicate very strong additional destabilization of η_i modes by unfavorable curvature found in RFP. In the pure g mode limit, the growth rate is $\gamma \sim \eta^{1/3}(-p_0'\kappa/B_0^2)^{2/3}(k_yL_s)^{2/3}$, and the mode width is $\lambda \sim \eta^{1/3}L^{2/3}k_y^{-1/3}(-p_0'\kappa/B_0^2)^{1/6}$, where $\kappa = 1/R_c$.

It is instructive to compare the η_i mode to the semi-collisional resistive interchange mode, the high temperature analogue of the g-mode. The ratio of mode widths $(\lambda_{\eta_i}/\lambda_{sc} \sim 10)$ indicates that pressure (and temperature) mixing due to η_i modes is much more significant than that due to the semi-collisional g-mode. Hence, it is likely that the η_i mode will dynamically dominate the semi-collisional resistive g-mode in high current RFP's.

V. Renormalized Equations

Consider the nonlinear evolution of a test η_i mode in the presence of a spectrum of multiple-helicity turbulence (due to other modes) in a sheared magnetic field. Fourier transforming in the y and z dimensions, the basic (convective) nonlinear interactions are

$$
\begin{aligned}
\left[\mathbf{b} \times \nabla\tilde{\phi} \cdot \nabla_\perp)\tilde{\tau}_i\right]_{\underline{\mathbf{k}}} &= i\left[\frac{\partial}{\partial x}\sum_{\mathbf{k}'} k'_y \tilde{\phi}_{-\mathbf{k}'}\tilde{\tau}_{i\mathbf{k}''} + k_y \sum_{\mathbf{k}'} \frac{\partial\tilde{\phi}_{-\mathbf{k}'}}{\partial x}\tilde{\tau}_{i\mathbf{k}''}\right] \\
&\quad - i\left[\frac{\partial}{\partial x}\sum_{\mathbf{k}'} k'_y \tilde{\tau}_{i-\mathbf{k}'}\tilde{\phi}_{\mathbf{k}''} + k_y \sum_{\mathbf{k}'} \frac{\partial\tilde{\tau}_{i-\mathbf{k}'}}{\partial x}\tilde{\phi}_{\mathbf{k}''}\right]
\end{aligned}
$$

etc., where $\mathbf{k}'' = \mathbf{k} + \mathbf{k}'$, and $\mathbf{k} = (k_y, k_z)$. The equations are renormalized by iteratively substituting the second order nonlinearly driven fields $\tilde{\phi}^{(2)}_{\mathbf{k}''}$, $\tilde{v}^{(2)}_{\| i\mathbf{k}''}$ and $\tilde{\tau}^{(2)}_{i\mathbf{k}''}$ for $\tilde{\phi}_{\mathbf{k}''}$, $\tilde{v}_{\| i\mathbf{k}''}$ and $\tilde{\tau}_{i\mathbf{k}''}$ respectively. The driven fields $\tilde{\phi}^{(2)}_{\mathbf{k}''}$ etc. are determined by the direct beat interaction of the test mode $\mathbf{k}$ with background $\mathbf{k}'$.[8] The result of this renormalization procedure can be schematically summarized by the substitution $\rho_s c_s\ (\mathbf{b} \times \nabla\tilde{\phi}) \cdot \nabla_\perp f \rightarrow -\frac{\partial}{\partial x}\left(D_{\mathbf{k}} \frac{\partial f}{\partial x}\right)$ in Eqs. (1)-(4), where random convection is replaced by turbulent diffusion:

$$
\begin{aligned}
&\left[\frac{\partial}{\partial t} + (1+\eta_i)V_{D_i}\frac{\partial}{\partial y} - \frac{\partial}{\partial x}D_{\mathbf{k}}\frac{\partial}{\partial x}\right]\rho_s^2\nabla_\perp^2\tilde{\phi} \\
&\qquad + V_C\frac{\partial}{\partial y}\left[(1+\tau)(\tilde{h}+\tilde{\phi}) + \tilde{\phi}_i\right] - \nabla_\|\tilde{j}_\|/ne = 0 \qquad (8)
\end{aligned}
$$

$$
\left(\frac{\partial}{\partial t} - \frac{\partial}{\partial x}D_{\mathbf{k}}\frac{\partial}{\partial x}\right)\tilde{v}_{\|i} = -v_{Ti}^2\nabla_\|\left[(1+\tau)(\tilde{h}+\tilde{\phi}) + \tilde{\tau}_i\right] + \nabla_\|(\mu_\|\nabla_\|\tilde{v}_{\|i}) \qquad (9)
$$

$$
\left(\frac{\partial}{\partial t} - \frac{\partial}{\partial x}D_{\mathbf{k}}\frac{\partial}{\partial x}\right)\tilde{\tau}_i = -\frac{2}{3}\nabla_\|\tilde{v}_{\|i} - \eta_i V_{De}\frac{\partial\tilde{\phi}}{\partial y} \qquad (10)
$$

$D_{\mathbf{k}}$ is defined as $D_{\mathbf{k}} = \sum_{\mathbf{k}'} k_y'^2 |\tilde{\phi}_{\mathbf{k}'}|^2/\Delta\omega_{\mathbf{k}''}$, and $(\Delta\omega_{\mathbf{k}''})^{-1}$ is the coherence time of modes $\mathbf{k}$ and $\mathbf{k}'$.

VI. Saturation Level

The saturation level can be estimated for high Reynolds number $R_e = (D_{\mathbf{k}}/\Delta_{\mathbf{k}}^2)/[\mu_{\|}(k_{\|}^2)_{\rm rms}\Delta_{\mathbf{k}}^2] \sim 0(\eta_i)$ by requiring balance of source with nonlinearity: $\partial E/\partial t = 0$. For the g-mode limit, the previous result[1,2] is modified by inclusion of dT_i/dx:

$$D \cong L_s^2\eta\left(\kappa + \frac{3}{2}\frac{\tau}{(1+\tau)L_{Ti}}\right)\beta_\theta/L_p.$$

For the η_i-mode ($\tilde{h} = 0$), it follows that

$$0 = \frac{\partial E}{\partial t} = -\frac{c}{eB}\left(\frac{T_i}{R_c} + \frac{3}{2}\frac{T_e}{(1+\tau)L_{Ti}}\right)\left\langle \tilde{T}_i \nabla_y \tilde{\phi}\right\rangle - \frac{1}{1+\tau}\left\langle \frac{\mu_{\|}}{v_{Ti}^2}|\nabla_{\|}\tilde{v}_{\|i}|^2\right\rangle.$$

For high Reynolds number, this mixing length estimate indicates that $D_{\mathbf{k}} \cong \left[1 + \frac{2}{3}(1 + \frac{1}{\tau})L_n/R_c\eta_i\right]^{1/2}\eta_i^2 v_{Ti} a_i^2 (k_y/a_i)_{\rm rms}/L_s$. In comparison to the pure η_i-mode limit, this result contains an extra driving term due to curvature $1/R_c$. A recent, more detailed (two point) theory of η_i mode turbulence yields the result[9] $D \cong (\pi/2)^2[\ell n(Re)]^2\eta_i^2 v_{Ti} a_i^2 (k_y a_i)_{\rm rms}/L_s$, where $(k_y a_i)_{\rm rms} \cong 0.4$. In that analysis, the interaction of gradient drive, nonlinearity, and sink (ion viscosity) was addressed in detail. Saturation occurs by nonlinear coupling to damped (by $\mu_{\|}$) short wavelength modes. In this more detailed calculation, it was shown that mixing length theory yields a good estimate of the mode saturation level.

VII. Transport Scaling

An estimate of η_i mode induced thermal conductivity can be obtained using the results obtained above: $\chi \cong (k_y a_i)_{\rm rms}\eta_i^2 a_i^2 v_{Ti}/L_s$, $\tau_{\rm ion} \cong a^2/\chi$. For $ZT-40$ parameters, taking $(k_y a_i)_{\rm rms} \sim 0.3$, $\eta_i \sim 2$, we find $\tau_{\rm ion} \cong 0.5$ msec, which lies within the range of current experimental results $0.3 < \tau_E < 0.7$ msec. For the case of rapid thermal equilibration $\tau_{eq} \sim \tau_E$, balance of thermal loss with Ohmic heating $\left(\tau_{\rm ion} = a^2/\chi = (NT)/(\eta I_p^2)\right)$ yields the scaling relation

$$T_e \sim I_p/N^{1/4} \sim (I_p/N)N^{3/4} \tag{11}$$

VIII. Summary and Suggestion

1. η_i modes can be strongly unstable in RFP, because of broad density profiles, ion heating, unfavorable average curvature, and strong shear.
2. η_i modes couple to g modes. The curvature and temperature gradient drives combine additively.
3. η_i modes are broader than, and thus dynamically supress, semi-collisional resistive interchange modes, when both are present.
4. Reynolds number estimates indicate that $\chi \sim \eta_i^2 a_i^2 v_{Ti}/L_s$, $(e\tilde{\phi}/T_e)_{\rm rms} \sim \eta_i^{3/2} a_i/L_s$.
5. η_i modes can be a major channel for thermal loss in high T and I_p RFP's. Confinement times $.3 < \tau_E < .6$msec are predicted for $ZT - 40$, and $T_e \sim I_p/N^{1/4}$ scaling is indicated.
6. Results 1-5 suggest that *pellet injection*[10] *is a potentially viable mechanism for improving energy confinement in the proposed high current RFP experiments.* Pellet injection is interesting for three reasons: a) to decouple I_p and N; b) to stabilize η_i modes by steepening of the density profile; c) to possibly reduce g-mode losses by driving the plasma into the $\omega_* > \gamma$ regime, where g-mode growth rates are reduced.[11] It may also be possible to achieve this end by low-Z impurity injection.[12]

Acknowledgments

The authors are grateful to T.S. Hahm for a useful discussion of the semi-collisional resistive interchange mode. This research was supported by the U.S. Department of Energy, contract no. DEFG05-80ET-53088.

References

1. Z.G. An, P.H. Diamond, and T.H. Chiueh, Proceedings of the Sixth U.S. Symposium on Compact Toroid Research, p. 259 (1984).
2. Z.G. An, P.H. Diamond, R.D. Hazeltine, J.N. Leboeuf, M.N. Rosenbluth, R.D.

Sydora, T. Tajima, B.A. Carreras, L. Garcia, T.C. Hender, H.R. Hicks, J.A. Holmes, V.E. Lynch, and H.R. Strauss, Paper IAEA-CN-44/E-III-10, Proceedings of the Tenth International Conference on Plasma Physics and Controlled Nuclear Fusion Research, London, 1984.

3. J.W. Conner and J.B. Taylor, Paper IAEA-CN-44/E-I-2, Proceedings of the Tenth International Conference on Plasma Physics and Controlled Nuclear Fusion Research, London, 1984.
4. R.S. Massey, Bull. Amer. Phys. Society **29**, 1228 (1984).
5. J.G. Cordey, E.M. Jones, and D.F.H. Start, Nucl. Fusion **20**, 459 (1980).
6. S.I. Braginskii, in Review of Plasma Physics, edited by M.A. Leontovich (Consultants Bureau, New York, 1965), Vol. 1, p. 205.
7. T.S. Hahm and L. Chen, PPPL-2185 (1985), accepted for publication in Phys. FLuids.
8. P.H. Diamond, et al., Phys. Fluids **27**, 1449 (1984).
9. G.S. Lee and P.H. Diamond, Paper 1S24, Sherwood Theory Meeting, 1985.
10. M. Greenwald et al., paper IAEA-CN-44/A-I-3, Proceedings of the Tenth International Conference on Plasma Physics and Controlled Fusion Research, London, 1984.
11. P.H. Diamond, et al., Phys. Fluids **28**, 1116 (1985).
12. E.A. Lazarus, et al., Nucl. Fusion **25**, 135 (1985).

Figure Captions

Fig. 1 Complex eigenfunction of pure η_i mode ($L_n/R_c = 0$) with $\eta_i = 4$, $k_y\rho_s = 0.3$, $T_e/T_i = 1$, $L_s/L_n = 2$, and negligible collisionality $\nu_e/\omega_{*e} = 0.001$.

Fig. 2 Complex potential for same mode and parameters as Fig. 1.

Fig. 3 Complex eigenfunction of coupled η_i and g modes ($L_n/Rc = 0.75$) with $\eta_i = 4$, $k_y\rho_s = 0.3$, $T_e/T_i = 1$, $L_s/L_n = 2$, and large collisionality $\nu_e/\omega_{*e} = 20$.

Fig. 4 Complex potential for same mode and parameters as Fig. 3.

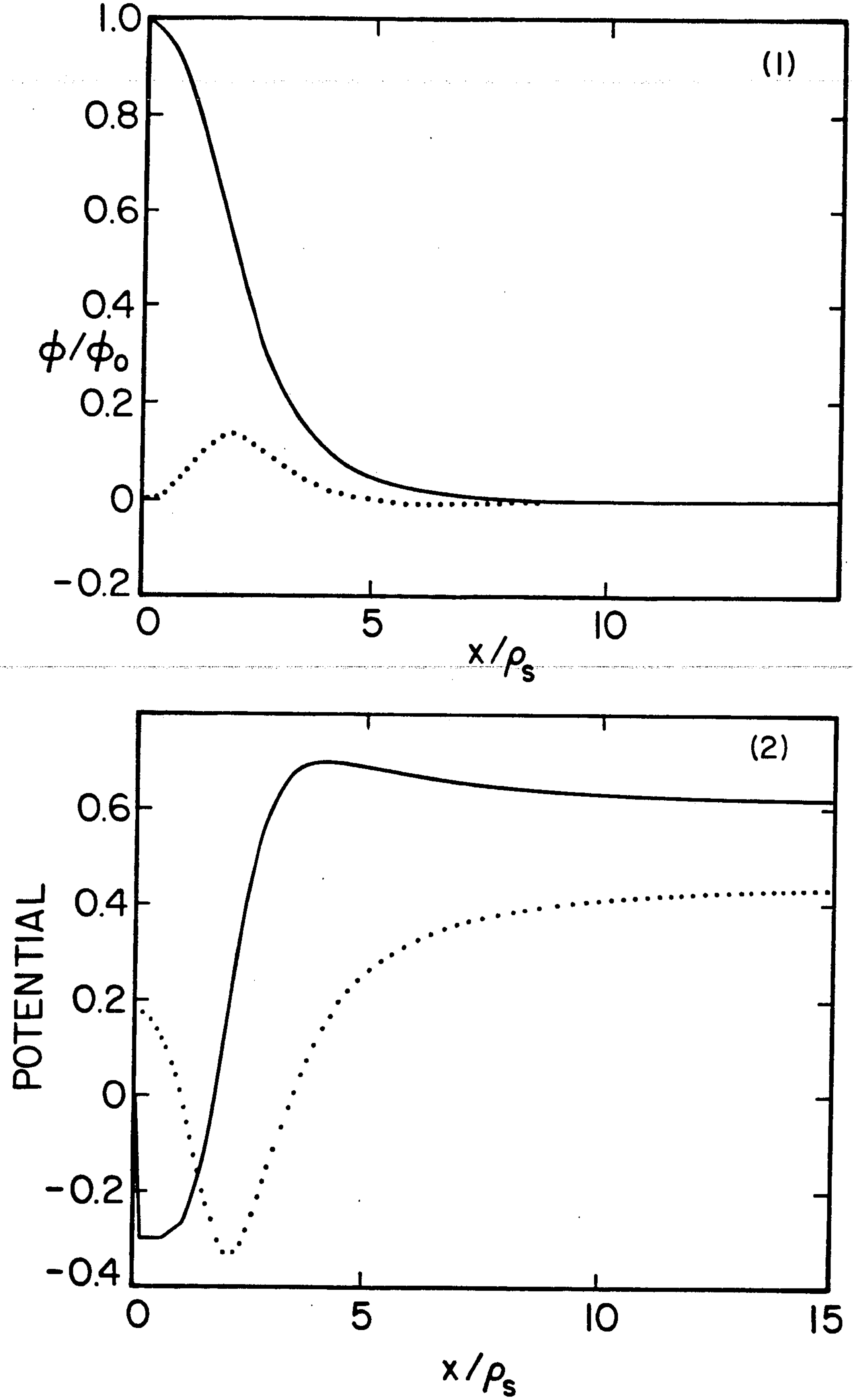

1.0
0.8
0.6
0.4
0.2
0
-0.2
φ/φ₀
(1)
0
5
10
x/ρs
0.6
0.4
0.2
0
-0.2
-0.4
POTENTIAL
(2)
0
5
10
15
x/ρs

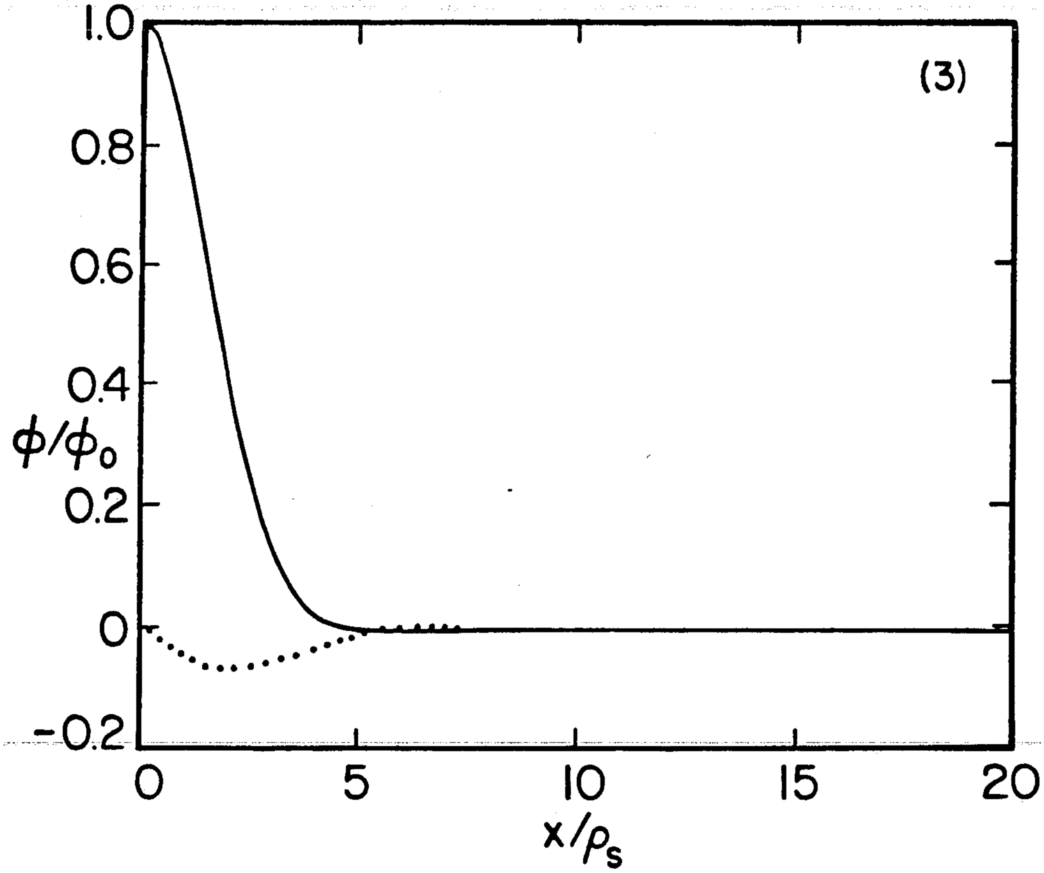

1.0
0.8
0.6
0.4
ϕ/ϕ_0
0.2
0
-0.2
(3)
0
5
10
15
20
x/ρ_s

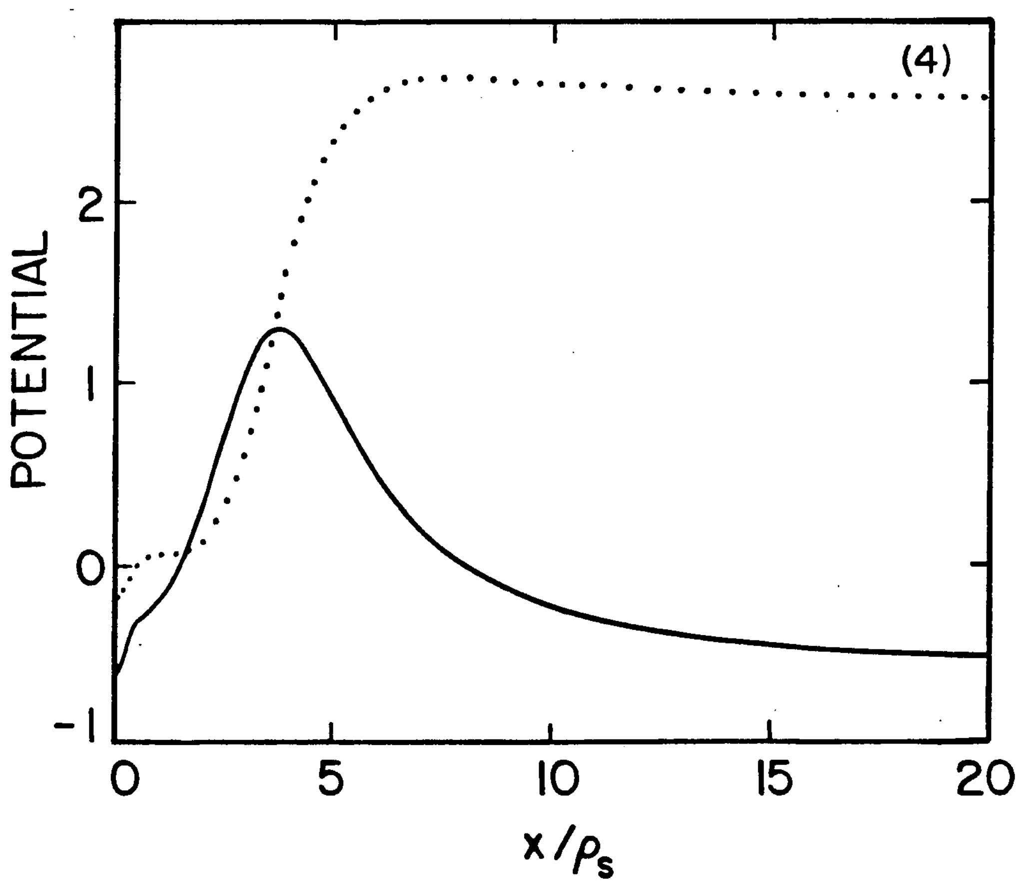

POTENTIAL
2
1
0
-1
(4)
0
5
10
15
20
x/ρ_s